RWM Modeling with VACUUM/NMA/DCON

M.S. Chance, M.S. Chu, M. Okabayashi, A.H. Glasser
PPPL, April 19, 2006

- Outline the structure of the code
- Some capabilities
- Won't present much results.
  Will present more when the fully up-down asymmetric version is debugged.

Main References:

- NMA (Normal Mode Analysis):
  M. S. Chu, M. S. Chance, A. H. Glasser and M. Okabayashi, *Nucl. Fusion*, **43**, 441-454 (2003).
- DCON:
  A. H. Glasser, and M. S. Chance, *Bull. Am. Phys. Soc.* **42**, 1848 (1997).
- VACUUM:
  M. S. Chance, *Phys. Plasma* **4**, 2161 (1997).

The Magnetic Scalar Potential with the Feedback Coils

- VACUUM solves for a surface response $\mathcal{C}_l(\theta_s)$ to the perturbation, $\mathcal{B}_l$, and the feedback coils, $\mathcal{I}_f$.
- For the plasma surface and either side $(-,+)$ of the resistive wall, on the:-

$$\text{plasma}:$$
$$\chi^p(\theta_p) = \sum_f \mathcal{C}_f^{pc-}(\theta_p)\mathcal{I}_f^- + \sum_{l_p} \mathcal{C}_{l_p}^{pp}(\theta_p)\mathcal{B}_{l_p}^p + \sum_{l_w} \mathcal{C}_{l_w}^{pw-}(\theta_p)\mathcal{B}_{l_w}^{w-} \tag{1}$$
$$\text{wall}^-:$$
$$\chi^{w-}(\theta_w) = \sum_f \mathcal{C}_f^{wc-}(\theta_w)\mathcal{I}_f^- + \sum_{l_p} \mathcal{C}_{l_p}^{wp-}(\theta_w)\mathcal{B}_{l_p}^p + \sum_{l_w} \mathcal{C}_{l_w}^{ww-}(\theta_w)\mathcal{B}_{l_w}^{w-} \tag{2}$$
$$\text{wall}^+:$$
$$\chi^{w+}(\theta_w) = \sum_f \mathcal{C}_f^{wc+}(\theta_w)\mathcal{I}_f^+ + \sum_{l_w} \mathcal{C}_{l_w}^{ww+}(\theta_w)\mathcal{B}_{l_w}^{w+}, \tag{3}$$

$\mathcal{C}_{l_{s'}}^{ss'}(\theta_{l_s})$ is the Fourier response coefficient matrix at θ_s at surface s due to the magnetic perturbation coefficients $\mathcal{B}_{l'_s}^s$ at surface s' and $\mathcal{C}_f^{ss'}(\theta_s)$ the response to the feedback coil coefficients, $\mathcal{I}_f^{+,-}$.

The Energies in the various regions

- The Green's Function technique allows the vacuum energies to be cast into terms involving quantities only on the bounding surfaces.

$$2E_v = \int_v |\nabla\bar{\chi}(\mathcal{Z},\theta',\phi')|^2\, dV \tag{4}$$
$$= \int_v \nabla\cdot(\bar{\chi}^*\nabla\bar{\chi})\, dV \tag{5}$$
$$= \int_S \bar{\chi}_p^*\nabla\bar{\chi}_p\cdot d\mathbf{S} \tag{6}$$
$$= \int_S \mathcal{C}^{*pq}\mathcal{B}^{*p}\mathcal{B}^q\cdot d\mathbf{S} \tag{7}$$

  using the relation, $\nabla^2\bar{\chi} = 0$, and Gauss's theorem.

- At first one needs only the potential on the surfaces surrounding each region external to the plasma

Cross-Section of the System – with Loops

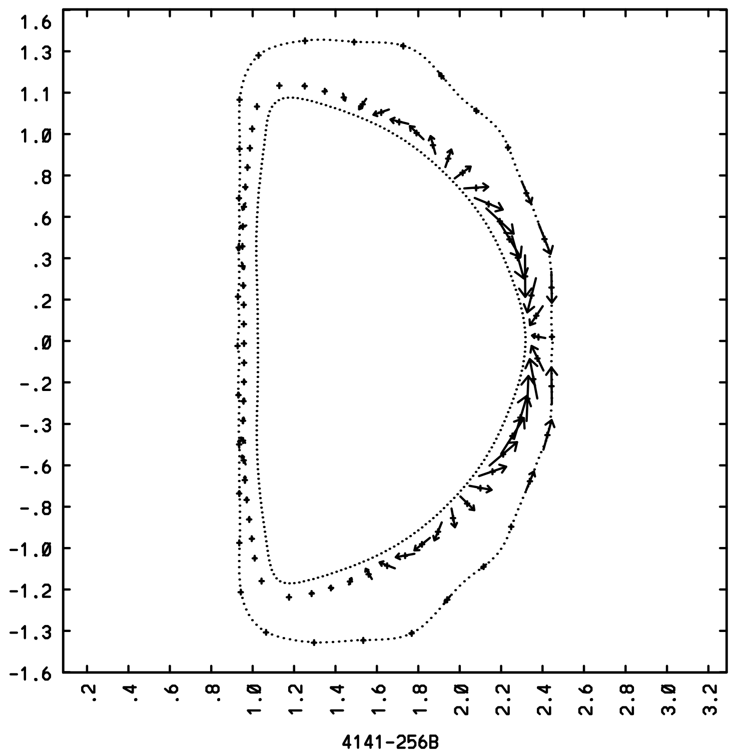

Figure 1: Magnetic perturbations in vacuum and on the shell.

Skin Current on the Shell

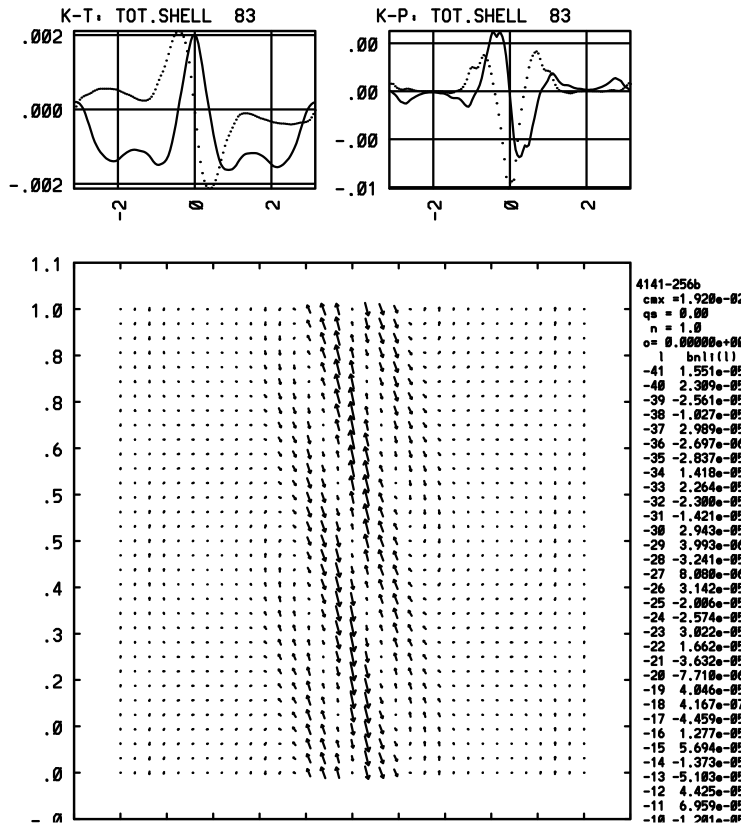

Figure 2: Rectilinear $\theta - \phi$ plot of the shell current.

B_θ and B_ϕ on the Shell

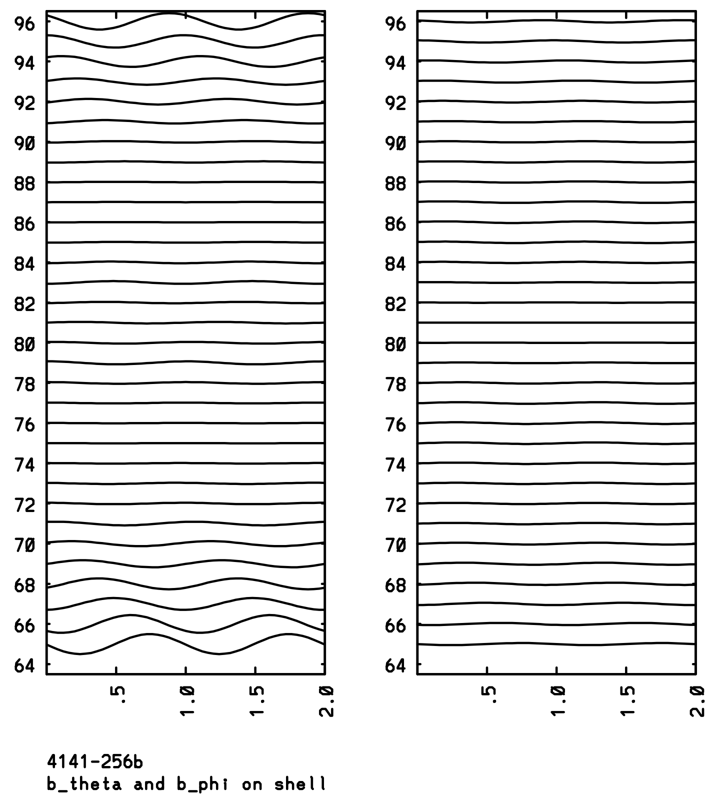

Figure 3: Loop magnetic fields on the shell as a function of ϕ.

B_θ and B_ϕ on the Shell – Constant Amplitude

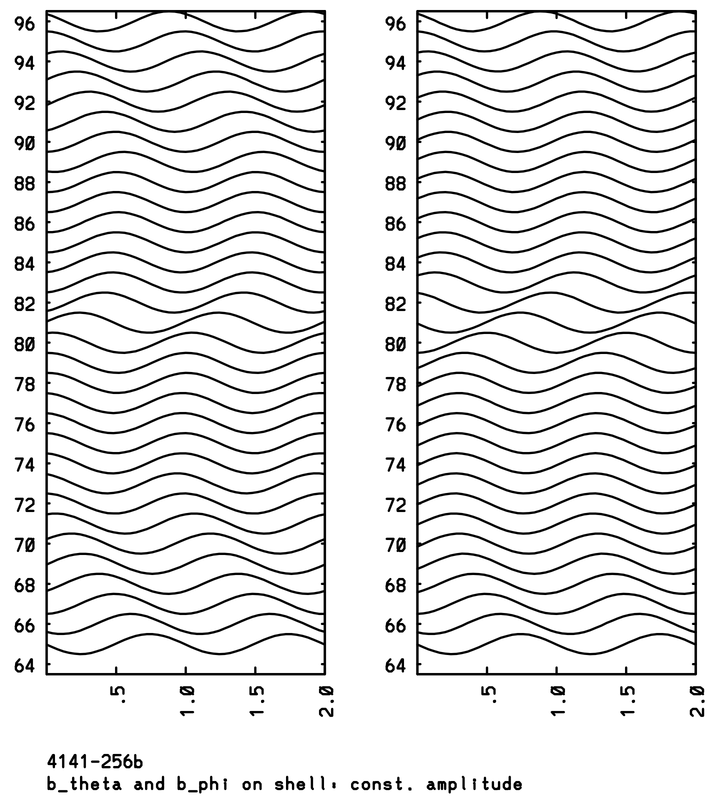

Figure 4: Plotted with constant amplitude to show loop phases.

The open loop eigenfunctions

- While we Fourier analyze in the toroidal angle ϕ, we used a complex representation for the plasma modes but decomposed the wall modes into even and odd solutions.

$$\mathcal{B}^p = [\mathcal{B}^p_r, \mathcal{B}^p_i] \tag{8}$$
$$\mathcal{B}^w = [(\mathcal{B}^w_{ec}, \mathcal{B}^w_{oc})\,(\mathcal{B}^w_{es}, \mathcal{B}^w_{os})] \tag{9}$$

  where the subscript 'c,s' denotes the part that multiplies the $\cos\phi$ and $\sin\phi$ in the representation.

- Double degenracy in the open loop energy matrix.
- In the up-down symmetric case one needs only $\mathcal{B}^p_r$, and $(\mathcal{B}^w_{ec}, \mathcal{B}^w_{os})$ to describe the system.
- Now we need all components to properly obtain the phase of the mode.

The open loop eigenfunctions

Without the feedback the energies can be cast into a self adjoint system with the dissipation in the shell playing the role of the energy norm.

$$\delta W_p(i,j) + \delta W_w(i,j) + \frac{1}{2}\sum_i \frac{\partial a_i}{\partial t} a_j^\dagger \delta_{ij} = 0 \tag{10}$$

where a_i is the amplitude of the resistive wall eigenfunction K_i, obtained by matching across the shell (using the thin shell approximation) and Faraday's and Ampere's laws:

$$\nabla_s \cdot [\eta |\nabla z|^2 \nabla_s K] = -|\nabla z|^2 \frac{\partial}{\partial t}\mathcal{B}_w \tag{11}$$

where K is the skin current stream function, z is a radial coordinate, $\eta(\theta)$ the resistivity, and $\mathcal{B}_w$ the normal magnetic field in the shell.

We set

$$\frac{\partial a_i}{\partial t} a_j = \gamma a_i a_j^\dagger . \tag{12}$$

Feedback

- Mode dynamics:

$$\frac{\partial \alpha_i}{\partial t} - \gamma_i \alpha_i = \sum_c E_i^c I^c \tag{13}$$

where

$$E_i^c = \int_w dS \chi_{fb}^c \frac{\partial \chi_i}{\partial n} \tag{14}$$

- Circuit equation:

$$\frac{\partial I_c}{\partial t} + \frac{1}{\tau_c} I_c = \sum_l G_c^l F_l \left(\{\alpha_i\}, \{I_c\}\right) \tag{15}$$

l is the index for the sensor loops, G_c^l is the amplication matrix, and F_l is the flux detected by the sensor loop l.

The I-coils of DIII-D

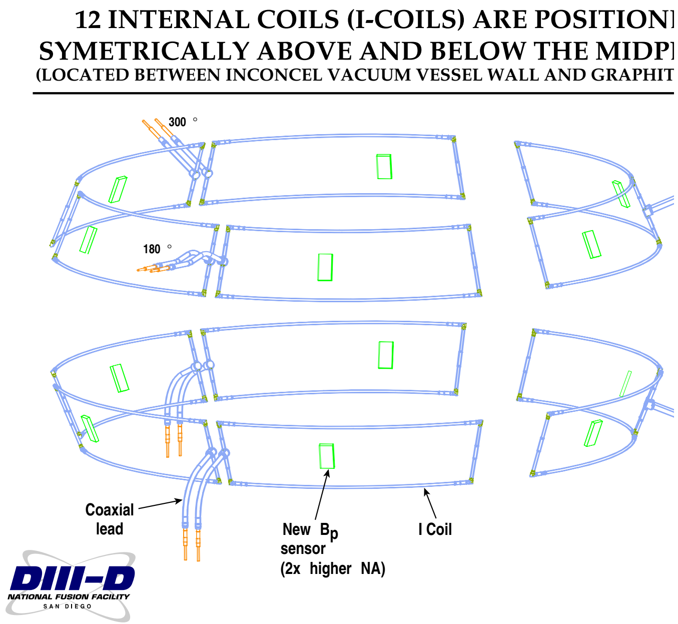

Figure 5:

Cross-section of the Plasma, Wall, Coils and a Sensor Loop

Upper coil:

	R_inner	R_outer
Actual:	2.164	2.374
Model:	2.159	2.369

	Z_bottom	Z_top
Actual:	0.5034	1.012
Model:	0.507	1.004

Lower coil: mirror imaged.

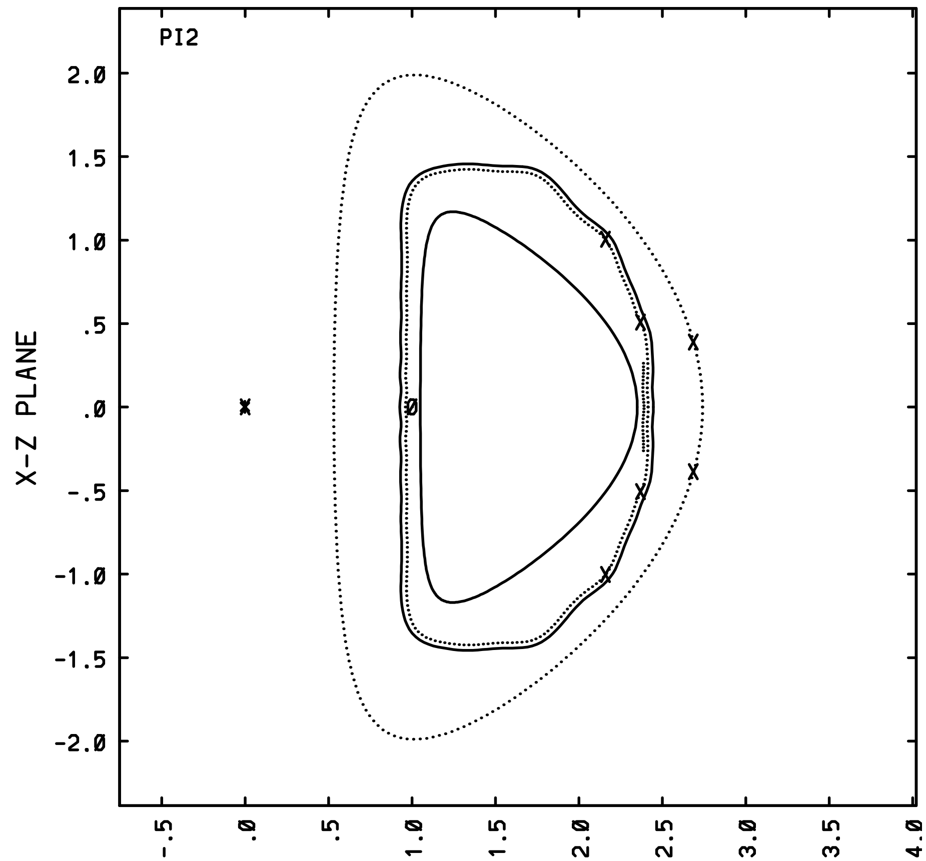

Potential Function for the DIII-D Feedback Coil

- Modeled accurately in the poloidal angle, θ.
- Approximately by a single harmonic in ϕ.

$$\mathbf{J}_f^c = \nabla \mathcal{Z} \times \nabla \chi_f(\theta, \phi) \delta(\mathcal{Z} - \mathcal{Z}_c). \tag{16}$$

$$J_{f\theta}^c = -\frac{|\nabla \mathcal{Z}|}{X} \frac{\partial \chi_f}{\partial \phi} e^{-in\phi}, \quad \text{and} \quad J_{f\phi}^c = \left(\frac{|\nabla \mathcal{Z}|^2}{X_\theta^2 + Z_\theta^2} \right)^{1/2} \frac{\partial \chi_f}{\partial \theta} e^{-in\phi}, \tag{17}$$

$[X(\theta), Z(\theta)]$ parameterizes the toroidally symmetric "shell" onto which each coil current is embedded.

For a "window-pane" coil centered at $\theta = 0$ and normalized to unity there is,

$$\chi_f(\theta, \phi) = \mathcal{I}_f \frac{1}{N_f} \frac{e^{[\cos\theta - \cos\theta_0]/\tau}}{e^{[\cos\theta - \cos\theta_0]/\tau} + 1} e^{-in\phi} \quad \equiv \quad \mathcal{I}_f \mathcal{F}_f(\theta, \phi), \tag{18}$$

where $N_f \equiv \exp\left[(1 - \cos\theta_0)/\tau\right] / \left(\exp\left[(1 - \cos\theta_0)/\tau\right] + 1\right)$,

- $\mathcal{I}_f$ is the complex amplitude of coil f.

Current distributions of the C and I coils

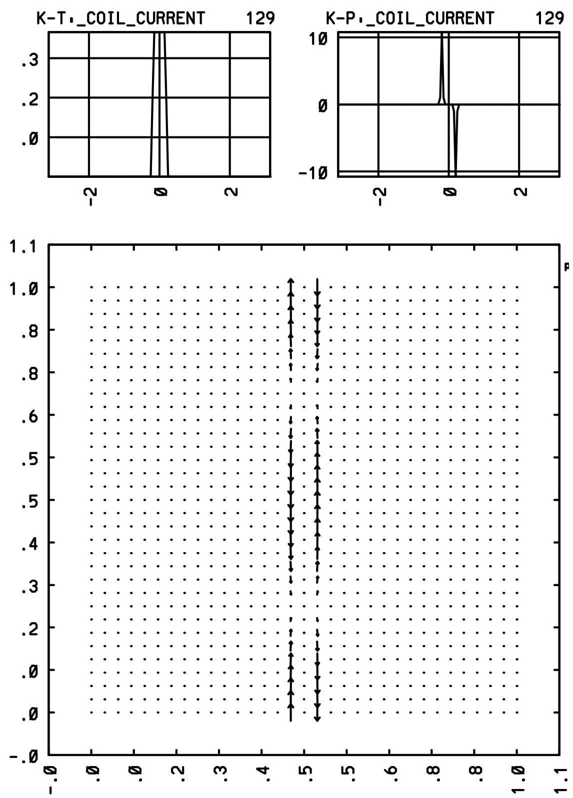

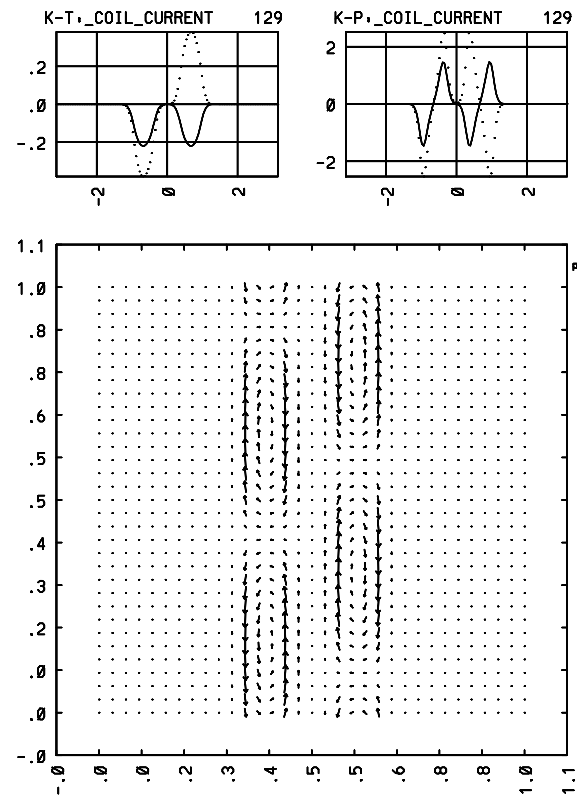

The C-Coil and I-Coils Current Distributions on the ϕ-θ plane with $\tau^{C}_{\mathrm{coil}} = 0.01$ and $\tau^{I}_{\mathrm{coil}} = 0.025$.
The relative phase is $4\pi/3$ which matches the unstable RWM at the coil locations

B_θ at the Plasma Surface due to the I-Coils

Centered coils. No phase shifts.

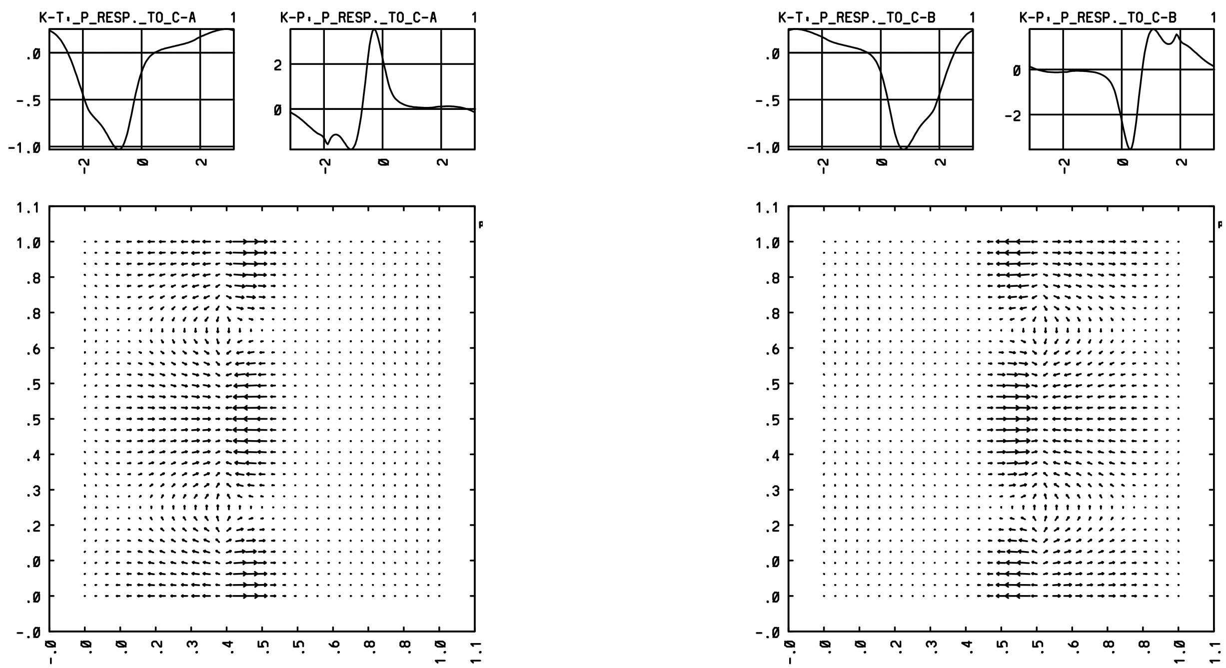

Figure 6: Tangential Field at the Plasma Surface due to Lower and Upper I-Coils

The Unstable RWM

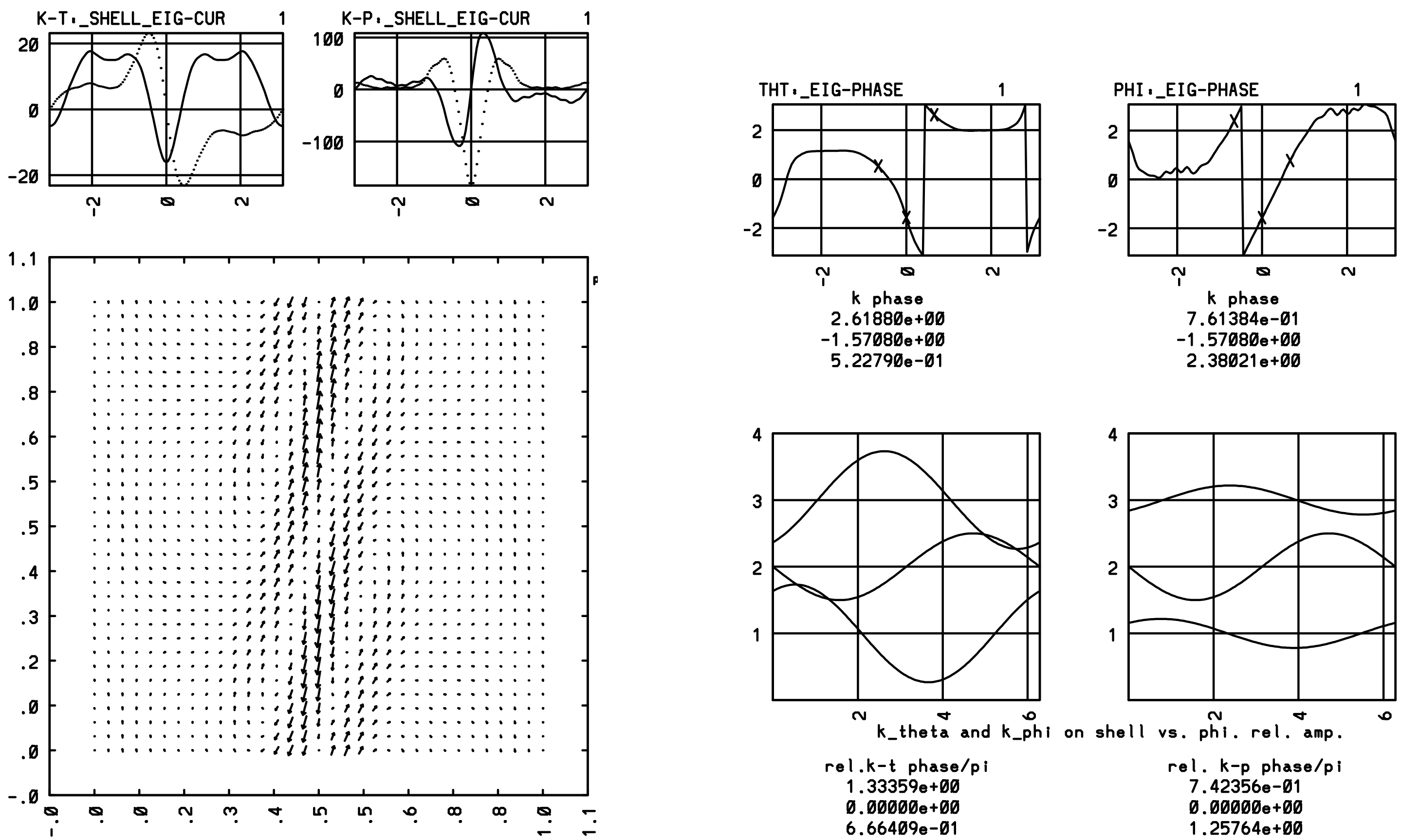

Figure 7: Current Distribution, Phase and Amplitiude on the Shell, of the unstable open loop eigenfunction.

Magnitude and Phase of the RWM at the I-Coil Positions

```
K-theta coil mag & phase       K-phi coil mag & phase
 1.46481E+00   2.61880E+00     4.35634E-01    7.61384E-01
 1.00000E+00  -1.57080E+00     1.00000E+00   -1.57080E+00
 1.46481E+00   5.22790E-01     4.35634E-01    2.38021E+00

             Rel.K-t phase/pi,  Rel. K-p phase/pi
                 1.33359E+00       7.42356E-01
                 0.00000E+00       0.00000E+00
                 6.66409E-01       1.25764E+00
```

The next two least stable eigenmodes

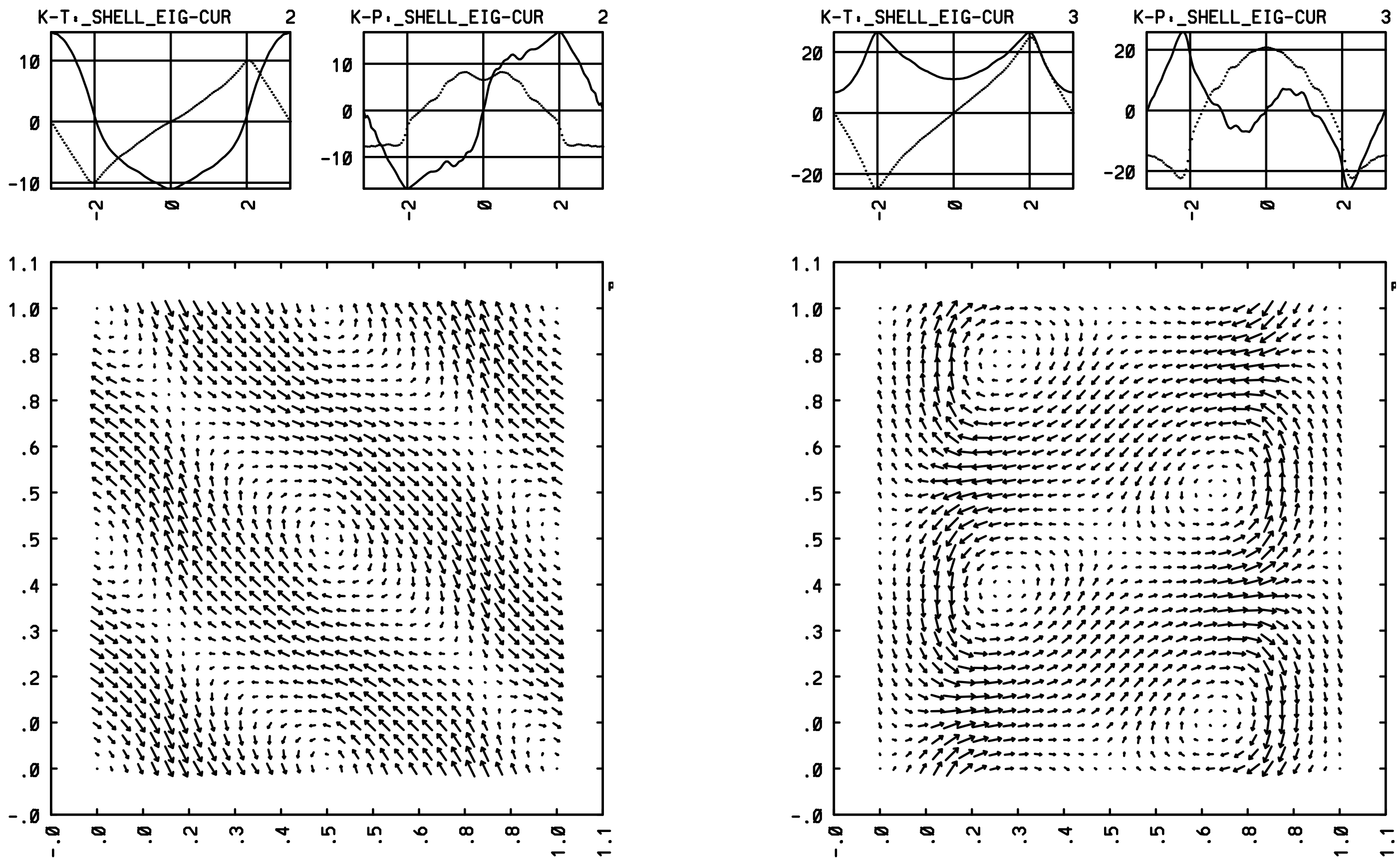

Figure 8: The next two (stable) open loop eigenmodes